Automatic Lineament Detection Using Digital Elevation Models with Second Derivative Filters

David Wladis

Abstract

A grid operator designed for the analysis of potential field data has been applied to a digital elevation model for the detection of lineaments. The results obtained have been evaluated using both an existing lineament map of the area and a field investigation. The evaluation indicates that the suggested methodology facilitates lineament detection. The high degree of consistency between the suggested method and the existing tectonic map indicates that lineaments in the study area are largely topographic features. Field validation confirmed these findings except in a few well-defined situations.

Introduction

In geology and hydrogeology, remote sensing is often used for the detection of brittle tectonic structures such as faults, large-scale fractures, and fracture zones. These structures are commonly denoted as lineaments (O'Leary *et al.*, 1976). Both satellite images and aerial photographs as well as other types of remote sensing data are used to detect lineaments. The technique can be used in applications such as groundwater exploration, prospecting for mineral and petroleum resources, hard rock engineering, and mapping of possible pathways for the transportation of pollutants.

In a lineament mapping procedure, the lineaments are often visually identified by an interpreter (e.g., a geologist), which implies that the obtained lineaments are in some way subjective interpretations and that they often are extracted manually, e.g., lineaments from the remote sensing data are hand-drawn on transparent overlays. This methodology produces results that to a large extent cannot be reproduced because the identification criteria are not agreed upon by different analysts and usually cannot be expressed in quantitative terms but, rather, are based on sensory impressions. Practically all geologic work includes some amount of subjective interpretation, but it is desirable to minimize this kind of uncertainty. Lineament extraction could be more highly valued if the results were reproducible. This would be achieved by using some form of automatic, or criteria-based, lineament extraction algorithm.

The idea of using different automated, or criteria-based, lineament-extraction algorithms is not new (Wang and Howarth, 1990; Moore and Waltz, 1983); however, several problems have arisen in the past. Slow algorithms and extensive manual editing have limited the use of such algorithms. Other approaches developed for optical data, such as aerial photographs and satellite images, often yield false lineaments that are related to roads, power lines, and other man-made features which are time consuming to correct (Gustafsson, 1994).

The Hough transform is frequently used to detect linear features in images (e.g., Karnieli *et al.*, 1993). The transform is computer intensive, and detected lines are extrapolated across the entire window, with the result that the direction of linear features rather than their spatial distribution is detected.

This paper suggests that a second vertical derivative filtering technique, in which the filter weights are optimized for the study region, be applied to digital elevation models (DEMs) for lineament detection. The digital filters employed were developed for analyses of potential field data such as magnetometry and gravimetry. By constructing second vertical derivative maps, qualitative and quantitative interpretations can be made more objective in the example of magnetic maps (Henderson and Zietz, 1967). The basic concept is that the data are convolved with a mathematical function in terms of a set of weights, which can be interpreted as a filter. The appropriate set of weights should be selected on the basis of its two-dimensional frequency response, which, in turn, may be data-dependent as discussed later.

In the study area, thorough lineament mapping was carried out by the Swedish Geological Survey (SGU) and presented as a tectonic map (Samuelsson, 1978). The mapping was done from aerial photographs at two scales. The SGU tectonic map facilitated the evaluation of the results obtained from the automatic detection, with respect to both spatial and directional distributions. A field study was also carried out, aimed primarily at examining the largest discrepancies between the automatically detected lineaments and the SGU tectonic map.

Digital Elevation Model

The DEM used here was produced by the National Land Survey (LMV). Three main sources for obtaining elevation data have been employed: aerial photographs, contour lines, and topographic profiles. Elevation data are used to interpolate elevation values on a regular grid with a spacing of 50 m. Because elevations in the DEM consist of interpolated values, the geometrical accuracy is less than that of directly measured points. The error is dependent on the interpolation algorithm and the topography of the specific area. However, the standard error of grid intersection points has been determined to be approximately ± 2 m (Ottoson, 1978). For further details on the establishment of the LMV DEM, refer to Ottoson (1978). The original DEM is shown in Figure 1.

In this context, the influence of the methodology used to produce the DEM (i.e., the interpolation algorithm) on the interpretability of lineaments should be considered. The accuracy of the interpolation of the grid nodes is affected by the relative relief of the area (Ottoson, pers. comm., 1996). However, the relative relief of the studied area is not considered

Department of Geology, Chalmers University of Technology, S-412 96 Gothenburg, Sweden (david@geo.chalmers.se).

Photogrammetric Engineering & Remote Sensing, Vol. 65, No. 4, April 1999, pp. 453–458.

0099-1112/98/6504–453$3.00/0

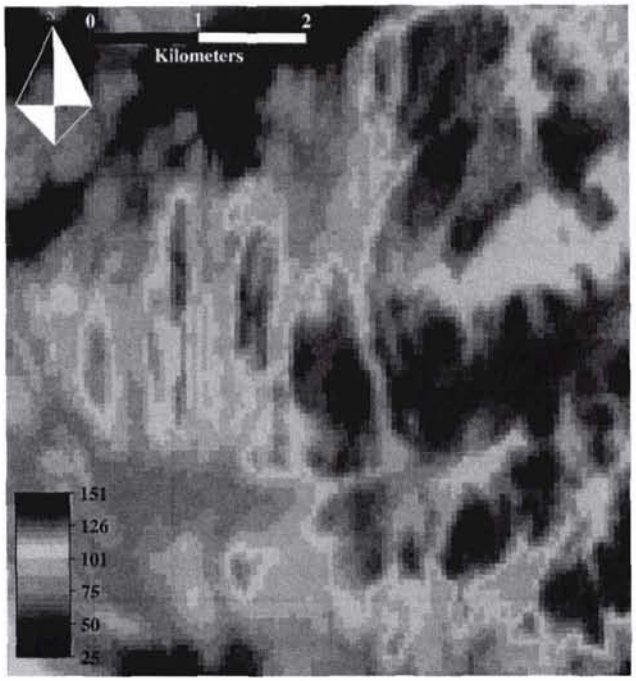

Figure 1. Original National Land Survey (LMV) DEM.

extreme compared to other parts of the country, and the accuracy of the DEM is considered to be high.

All image processing of the DEM is carried out using a standard image processing system, ERMapper 5.0. Subsequent analyses were carried out in a geographical information system, Genamap 4.2.

Filtering Technique

Elevations and other potential field data (e.g., magnetic maps) are often represented on a regular grid, so equations and formulas developed for the analysis of potential field data are readily applied to DEMs.

Different kinds of grid operators are designed to accomplish specific purposes on potential field data (e.g., to remove trends or to study features of small areal extent). These grid operators may be interpreted as filters with frequency responses in a two-dimensional frequency domain (Fuller, 1967). A variety of methods have been developed for use in analyses of gravitational and magnetic data, but, for the purposes of this study, a derivative method has been applied. The theory and design of the grid operators used in this method are described in Båth (1974) and Fuller (1967). In this study, the grid operators chosen were the second vertical derivative operators described by Henderson and Zietz (1967).

Lineaments in a digital elevation model are defined by a drop in elevation for a short distance. Therefore, a lineament can be described by a certain frequency in terms of its representation in a digital elevation model. Consequently, we are interested in the frequency domain of the sampled data and, thus, the frequency response of the filter.

The essential equations in Henderson and Zietz (1967) for the computation of filter constants are described next. The equations are derived in Henderson and Zietz (1967), who provide the following series expansion:

$$\overline{\Delta T}(r) = \sum_{k=1}^{k} A_k J_0(\mu_k r) \qquad (1)$$

where $\overline{\Delta T}$ represents the average value of ΔT (total intensity) on the circle of radius r, J_0 is a Bessel function of zero order, A_k are coefficients to be determined, and μ_k are positive roots of $J_0(\mu_k r)$.

In order to compute the second vertical derivative of the total intensity (ΔT) at the origin, the following equation is provided:

$$\frac{\partial^2 \Delta T}{\partial z^2} = \sum_{k=1}^{k} \mu_k^2 A_k J_0(\mu_k 0) = \sum_{k=1}^{k} \mu_k^2 A_k \qquad (2)$$

where the coefficients A_k can be computed by solving K equations in K unknowns, which involves the value of the anomaly at the center and the average values of ΔT on $K - 1$ circles about the origin. This is illustrated in Figure 2.

From Equation 1, the following simultaneous equations are used to solve for the coefficients in order to compute the filter for a nine-point convolution matrix consisting of ΔT_0 and eight neighboring points:

$$\begin{aligned} \Delta T_0 &= A_1 + A_2 + A_3 \\ \overline{\Delta T_1} &= A_1 J_0(\mu_1 r_1) + A_2 J_0(\mu_2 r_1) + A_3 J_0(\mu_3 r_1) \\ \overline{\Delta T_2} &= A_1 J_0(\mu_1 r_1) + A_2 J_0(\mu_2 r_2) + A_3 J_0(\mu_3 r_2) \end{aligned} \qquad (3)$$

Then $r_1 = S$ and $r_2 = S\sqrt{2}$ (where S is the grid spacing), if the averaging circles are transformed to cartesian coordinates (Fuller, 1967) as shown in Figure 2. To solve for the coefficients A_1, A_2, A_3 in Equations 3, we take $10S$ as the radius at which the idealized anomaly is arbitrarily smoothed to zero, i.e., where ΔT is essentially zero (Henderson and Zietz, 1967). Equation 2 can then be written as

$$\frac{\partial^2 \Delta T}{\partial z^2} = (6.185\Delta T_0 - 8.374\Delta T_1 + 2.189\Delta T_2)\frac{1}{S^2} \qquad (4)$$

which is the working formula. In this study, different sizes of filters have been computed and tested on the DEM. The grid operators for different filter sizes have been computed using Matlab 4.2a.

The degree of detail in the final result is achieved mainly by modifying the threshold value, which is described

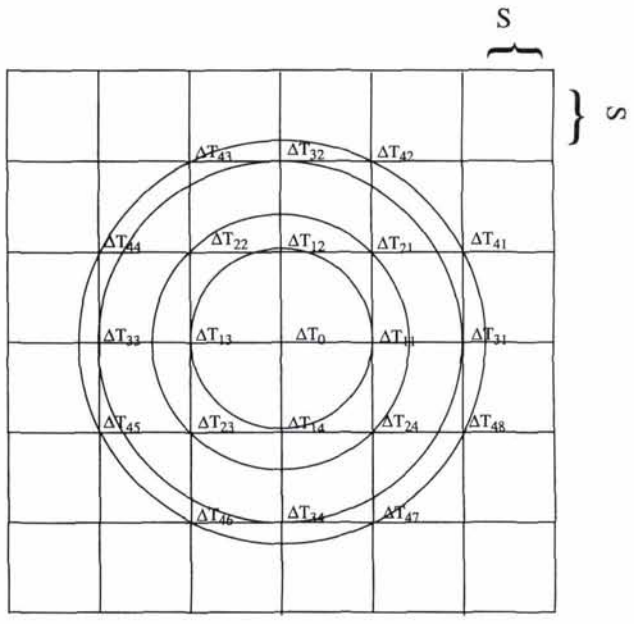

Figure 2. Graphical relation between averaging rings, $\Delta T(r)$, and Cartesian coordinate points, ΔT.

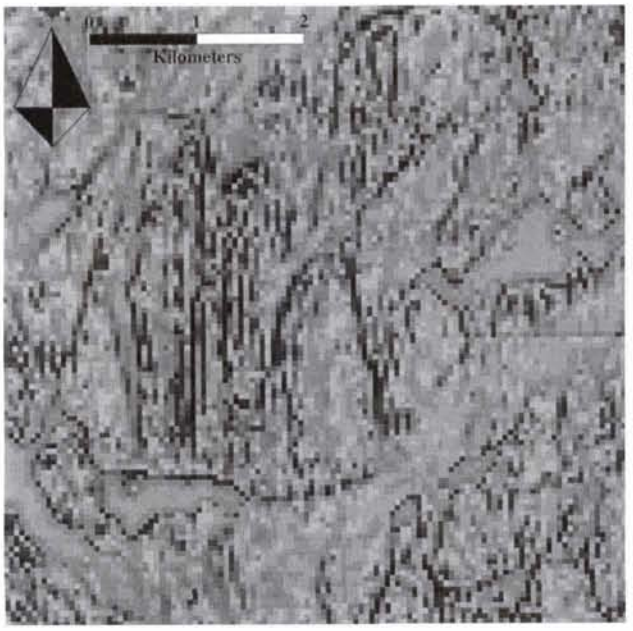

Figure 3. National Land Survey (LMV) DEM filtered using second vertical derivative filter.

in the following section. The detection limit of structures (i.e., the cut-off limit) is governed not by the filter size but by the characteristics of the filter function. For larger filter sizes, the detection frequency is better defined. The filter yields values of sufficient accuracy for a 3 by 3 filter matrix in the geomagnetic example described by Henderson and Zietz (1967). In order to study and compare the effect of different grid operators, frequency analysis can be used (Fuller, 1967).

The grid spacing may also influence the results. A fine grid spacing produces more accurate results in terms of degree of detail. However, for certain purposes, only the regionally developed lineaments are of interest. By increasing the grid spacing in proportion to the size of the structures to be studied, minor and local structures can be removed (Henderson and Zietz, 1967).

The size of the filter matrix is proportional to the wavelengths allowed through the filter (Mather, 1987). Therefore, broader structures are detected using a larger filter size, given that they yield a sufficiently high frequency. A filter of this type produces a margin around the image proportional to the size of the filter matrix. This margin contains no data. For a 5 by 5 filter, the margin is two pixels whereas, for a 21 by 21 filter, the margin is ten pixels broad. Therefore, a smaller filter may be preferable. It is worth noting that larger filters are more computer intensive.

A listing of how the grid operators were computed in Matlab 4.2a is provided in the appendix. The listing is in the form of a Matlab script file, including the statements and data necessary to compute a 5 by 5 filter. The script can be edited in order to compute an arbitrary filter size. The computed grid operators are used to convolve the DEM. This operation is implemented in all raster-based image processing systems, e.g., ERMapper. The filtered output is shown in Figure 3.

Threshold

The thresholding procedure is applied to extract the relevant information from the filtered output. The threshold value can be set to obtain the desired degree of detail. In areas where the structures range from narrow fracture zones to broad valleys, the applied threshold value may be crucial. By adjusting the threshold properly, classification of the structures based on their prominence is also possible. Classification of lineaments is performed manually in the compilation of tectonic maps (Ottoson, 1978).

In the filtered image, topographic lows occur as negative pixel values and topographic highs as positive pixel values, i.e., the extremities of the slopes in the original DEM are picked out by the filter. The magnitude of the value is proportional to the gradient of the slope. Lineaments are represented by some specific level of the negative pixel values. Therefore, it is convenient to threshold the image. Generally, the threshold can be set using either of the following methods. Using existing data, the threshold value can be calibrated from a few known structures in the area or from an existing tectonic map. Unfortunately, such data are not always available. The threshold may also be set using professional judgement. To some extent, this introduces subjectivity into the mapping process, but the mapping of structures is consistent throughout the area and the results are reproducible.

Thresholding of the image also provides line thinning. In this instance, pixels ≤ -5 were set to 255 (gray in Figure 4) and all other pixels to 0 (white in Figure 4). The resulting image is shown in Figure 4. Single pixels and minor clusters of pixels still remain in the image. These pixels represent high frequency features of small areal extent such as small lakes and pits.

Validation of Results

The most time-consuming aspect of studies comprising extraction of lineaments is evaluating and validating results in the field. Fortunately, a comparison of the results obtained with an existing tectonic map was possible. Furthermore, in this restricted pilot study, a thorough field examination was considered to be an important component.

A tectonic map of the study area was published by SGU (Samuelsson, 1978), where lineaments were interpreted from aerial photographs of two different scales, 1:33,000 and 1:65,000. A systematic control in the field of the lineaments obtained has not been undertaken by SGU. However, the degree of error of the mapped lineaments is empirically estimated by Samulesson (1978) at less than 1 percent (i.e., fewer than 1 percent of the mapped structures lack field evidence). The results of Samuelsson (1978) were compared to those obtained from the DEM.

The lineaments extracted from the DEM provide a useful map for different geological applications (Figure 4) but, for the purposes of this study, they were vectorized by on-screen digitizing using two conditions: (1) a lineament consists of at least four pixels (200 m) and (2) there cannot be a gap of more than one pixel (50 m) between any two groups of at least four pixels, criteria that can easily be automated. The map containing the digitized lineaments is shown in Figure 5. It should, however, be noted that the lineaments are digitized mainly to facilitate the preparation of lineament statistics and that the digitizing procedure may lead to at least some loss of information.

The lineaments obtained from the DEM and lineaments from the SGU map were plotted in separate histograms (Figure 6). From the histograms, it can be seen that the north- and northeast-trending lineament directions are dominant in both extraction procedures.

The lineaments from the SGU tectonic map and the automatically extracted lineaments are summarized in Tables 1 and 2, respectively. The lineaments are sorted in 5-degree intervals. From the tables, it is clear that the three largest peaks determined using each procedure coincide except for a

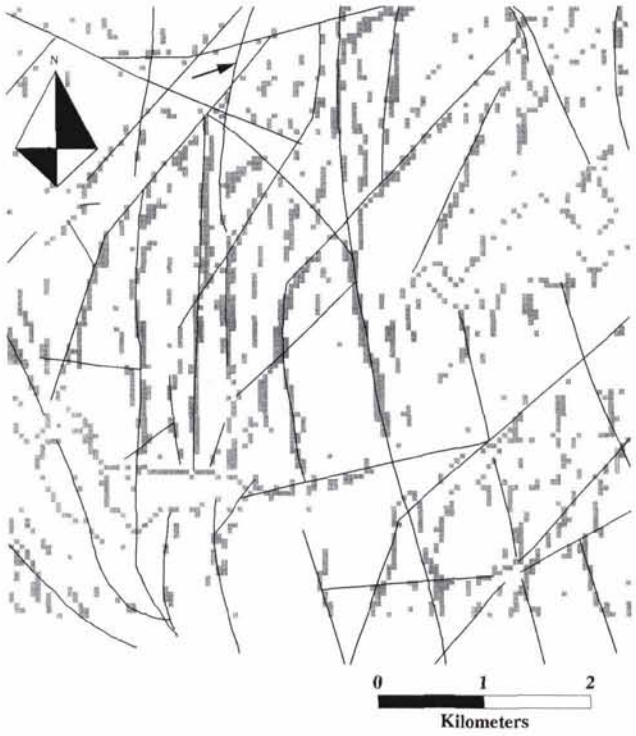

Figure 4. Automatically extracted lineaments in raster format (gray) overlaid by SGU lineaments (black lines).

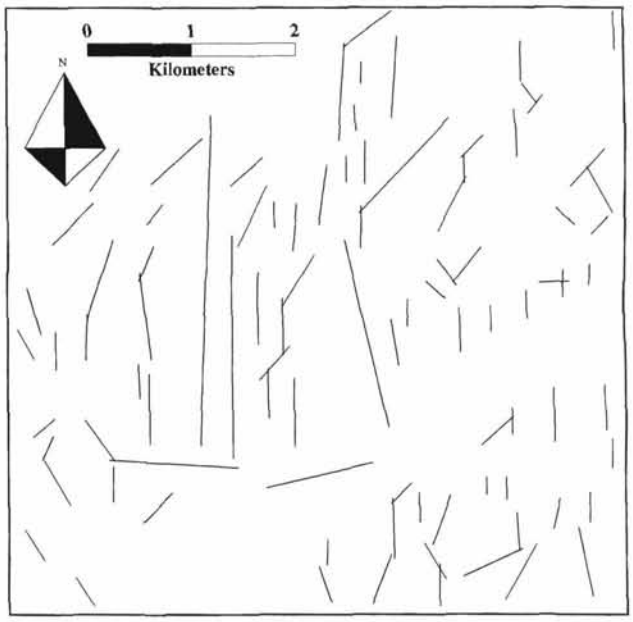

Figure 5. The digitized, automatically extracted lineaments from the DEM.

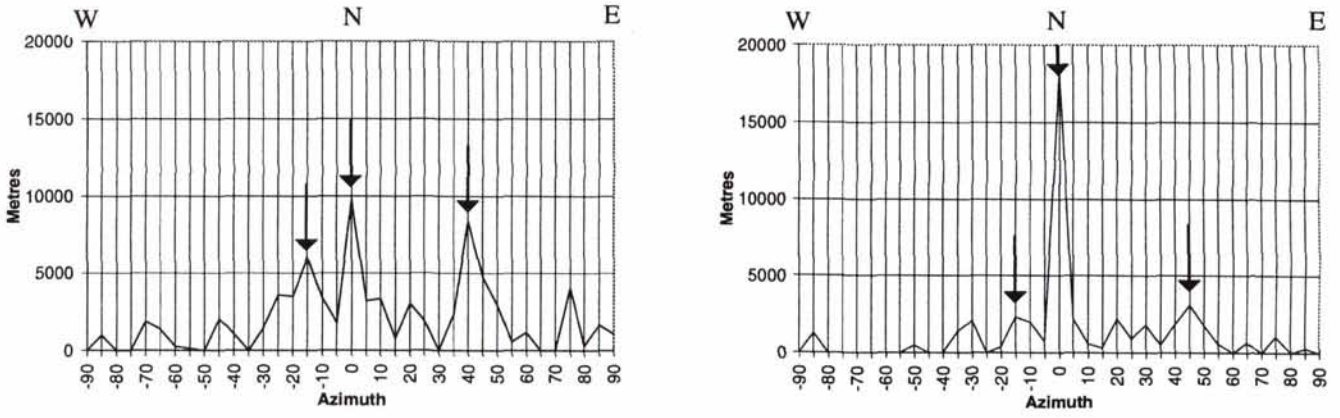

Figure 6. Lineaments extracted by SGU (left), and from DEM. Arrows indicate three largest peaks.

TABLE 1. SGU LINEAMENTS: FOUR MOST PROMINENT TRENDS (LENGTH IN METRES)

Azimuth	Frequency	Min. Length	Max. Length	Mean Length	Total Length	Mean Angle
NS	11	258.1	3307.5	886.5	9751.1	N 0.3° E
N 40° E	7	376.9	2447.3	1196.8	8377.9	N 40.7° E
N 15° W	9	248.4	1347.8	667.0	6002.7	N 14.3° W
N 45° E	2	1568.0	3164.7	2366.3	4732.6	N 44.9° E

TABLE 2. AUTOMATICALLY EXTRACTED LINEAMENTS: FOUR MOST PROMINENT TRENDS (LENGTH IN METRES)

Azimuth	Frequency	Min. Length	Max. Length	Mean Length	Total Length	Mean Angle
NS	37	175.3	3193.2	494.0	18278.5	N 0.4° W
N 45° E	6	241.4	1272.0	513.1	3078.6	N 43.8° E
N 15° W	2	470.0	1856.9	1163.4	2326.9	N 14.6° W
N 5° E	3	462.6	942.4	733.2	2199.6	N 3.8° E

small discrepancy, i.e., the second-largest peak is in the N40°E interval in the SGU lineaments, whereas it is in the N45°E interval in the DEM lineaments. But the tables show that the mean discrepancy is only 3 degrees. The peak at N15°W in Table 2 (DEM data) consists of only two lineaments.

Field Evaluation

The field examination was aimed mainly at evaluating differences between the two mapping methods. In the lineaments mapped by SGU, lineaments were systematically interpolated and extrapolated. This is particularly clear in paved and landfilled areas, where no trace of lineaments could be found in the field. Furthermore, lineaments shorter than approximately 250 m were not recognized by SGU. Lineaments represented by a "step" or a broad valley tend to be under-represented in the automatic mapping procedure. Under-representation of narrow structures is possibly connected to the resolution of the DEM, which is about ten times less than that of the aerial photographs used by SGU. A prominent, slightly curvilinear lineament mapped by SGU (indicated by an arrow in Figure 4) was not mapped in the automatic procedure.

Conclusions

The lineaments detected coincide largely with the lineaments mapped by SGU in terms of strike directions. Discrepancies detected in the field favor the automatically detected lineaments except for two situations, i.e., when the mapped lineaments are slightly curvilinear or when they are represented by "steps" in the terrain. Therefore, it can be concluded that the suggested technique extracts appropriate lineaments from DEMs. The resolution of the DEM and the behavior of the algorithm when applied to curvilinear lineaments should be considered. The results also suggest that lineaments in this area, to a large extent, are represented by topography.

A threshold value can be applied to produce the most suitable output for the intended use. The output map may range from only the largest structures of regional impact to all structures, including the smallest structures inherent in the original data. Furthermore, the criteria applied in the digitizing procedure is arbitrary. As pointed out above, the raster-to-vector data conversion may cause a reduction in the information content in the final map. Therefore, the chosen criteria for digitizing is dependent on the intended application. In this study, results are based exclusively on elevation data. Integrating other data such as satellite data and aerial photographs, if available, may further improve results.

Acknowledgments

The Swedish National Space Board is gratefully acknowledged for the funding of this project. Thanks are due to Professor Mike Middleton and Erik Larsson at the Department of Geology, Chalmers University of Technology, for guidance at various stages of the work.

References

Båth, M., 1974. *Spectral Analysis in Geophysics: Developments in Solid Earth Geophysics 7*, Elsevier Scientific Publ. Co., Amsterdam, 563 p.

Fuller, B.D., 1967. *Two-dimensional frequency analysis and design of grid operators, Mining Geophysics, Volume II, Theory*, Society of Exploration Geophysicists, Tulsa, Oklahoma, pp. 658–08.

Gustafsson, P., 1994. SPOT satellite data for exploration of fractured aquifers in a semi-arid area in southeastern Botswana, *Applied Hydrogeology*, 2(2):9–18.

Henderson, R.G., and I. Zietz, 1967. The computation of second vertical derivatives of geomagnetic fields, *Mining Geophysics, Volume II, Theory*, Society of Exploration Geophysicists, Tulsa, Oklahoma, pp. 606–20.

Karnieli, A., A. Meisels, L. Fisher, and Y. Arkin, 1993. Automatic extraction and evaluation of geological linear features from digital remote sensing data using a Hough transform, *Proc. 9th Environmental Research Institute of Michigan Thematic Conference on Geologic Remote Sensing*, Pasadena, California, pp. 299–310.

Mather, P.M., 1987. *Computer Processing of Remotely-Sensed Images*, John Wiley & Sons, Chichester, 352 p.

Moore, G.K., and F.A. Waltz, 1983. Objective procedures for lineament enhancement and extraction, *Photogrammetric Engineering & Remote Sensing*, 49:641–647.

O'Leary, D.W., J.D. Friedman, and H.A. Pohn, 1976. Lineaments, linear, lineations: Some proposed new standards for old terms, *Geol. Soc. Am. Bull.*, 87:1463–1469.

Ottoson, L., 1978. Establishment of a high density terrain elevation data base in Sweden, *Proc. 9th International Conference on Cartography*, International Cartographic Association, Maryland, in National Land Survey (Lantmäteriverket) Professional Papers, Gävle, Sweden, 15 p.

Samuelsson, L., 1978. *Description of the Map of Solid Rocks Göteborg SO*, Sveriges Geologiska Undersökning, serie Af, no. 117, map scale: 1:50,000, Stockholm, Sweden, 85 p.

Wang, J., and P.J. Howarth, 1990. Use of the Hough transform in automated lineament detection, *IEEE Trans. on Geoscience and Remote Sensing*, 28(4):561–566.

(Received 15 September 1997; accepted 09 April 1998; revised 25 May 1998)

Appendix

```
%%%% This is the Matlab script file %%%%

        %% positive roots to J0(μk r) %%

root=[2.4048255577  5.5200781103  8.6537279129  11.7915344391  14.9309177086
18.0710639679]

        %% Circle radius, r %%

radii=[0 1 sqrt(2) 2 sqrt(5) sqrt(8)]

        %% compute J0(μi rj) and put them in a matrix %%

for i=1:6;
 for j=1:6;
  mat(i,j)=besselj(0,root(i)*radii(j)/10);
 end
end

        %% Solve the simultaneous equations (3) %%

A=inv(mat)*(root.*root)'/100

        %% transform Ak to cartesian coordinates %%

b=A.*[1 1/4 1/4 1/4 1/8 1/4]'

        %% The grid operators organised in a convolution matrix %%

c(3,3)=b(1);
c(2,2)=b(3);
c(1,1)=b(6);
c(3,2)=b(2);
c(2,3)=b(2);
c(1,3)=b(4);
c(3,1)=b(4);
c(1,2)=b(5);
c(2,1)=b(5);
```

```
for j=1:3
for i=4:5
c(j,i)=c(j,6-i);
 end
end

for i=4:5
for j=1:5
c(i,j)=c(6-i,j);
 end
end
c
```

%%%% Which will create the following output %%%%

```
root =
    2.4048    5.5201    8.6537   11.7915   14.9309   18.0711
radii =
    0.0000    1.0000    1.4142    2.0000    2.2361    2.8284
A =
    8.5254
   -16.1224
    9.9515
   -4.1796
    1.8875
   -0.0625
b =
    8.5254
   -4.0306
    2.4879
   -1.0449
    0.2359
   -0.0156
c =
   -0.0156    0.2359   -1.0449    0.2359   -0.0156
    0.2359    2.4879   -4.0306    2.4879    0.2359
   -1.0449   -4.0306    8.5254   -4.0306   -1.0449
    0.2359    2.4879   -4.0306    2.4879    0.2359
   -0.0156    0.2359   -1.0449    0.2359   -0.0156
```